JOC The Journal of Organic Chemistry

Article

pubs.acs.org/joc

A Perspective on Designing Chiral Organic Magnetic Molecules with Unusual Behavior in Magnetic Exchange Coupling

Prodipta Sarbadhikary,[†] Suranjan Shil,[‡] Anirban Panda,[§] and Anirban Misra*[,†]

[†]Department of Chemistry, University of North Bengal, Dist-Darjeeling 734013, India

[‡]Institute for Inorganic and Applied Chemistry, University of Hamburg, Martin-Luther-King-Platz 6, 20146 Hamburg, Germany

[§]Department of Chemistry, J. K. College, Purulia PIN-723101, West Bengal, India

Supporting Information

ABSTRACT: A total of nine diradical-based organic chiral magnetic molecules with allene and cumulene couplers have been theoretically designed, and subsequently, their magnetic property has been studied by density functional theory. It is found that with an increase in length of the coupler, a remarkable increase in spin density within the coupler takes place. An increase in the length of the coupler reduces the energy of LUMO, and a smaller HOMO−LUMO gap facilitates stronger magnetic coupling and thereby a higher magnetic exchange coupling constant (J). This observation is supported by the occupation number of natural orbitals.

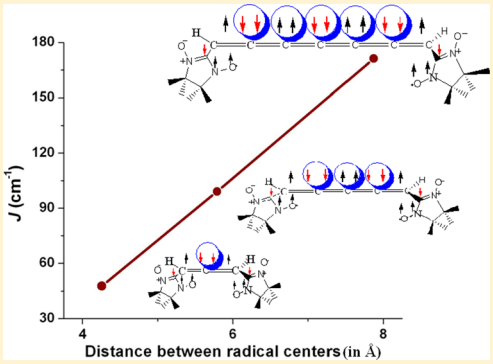

1. INTRODUCTION

Chirality is of utmost importance as it plays a key role not only in life forms but also in pharmaceutical, agricultural, and other chemical industries.[1] At present, chiral organic molecules are of great interest to organic chemists as well as pharmaceutical chemists.[2] Galán-Mascarós et al. have synthesized molecular materials with ferromagnetism, metal-like conductivity, and chirality.[3] When chirality appears in the structure of atoms in a solid that has unpaired electrons, the chiral lattice favors a screwlike arrangement of the magnetic moments of unpaired electrons, but they must compete with ferromagnetic exchange, which attempts to align all the magnetic moments in the same direction. These chiral lattices are known as chiral magnets.[4] On the other hand, chiral magnetic molecules with ferromagnetic interaction can also be regarded as chiral magnets.[5] Stable chiral magnets are important ingredients for future data storage, spintronic devices,[6] and other applications for their fascinating properties.[4] The most important phenomena shown by chiral magnets are the magneto-chiral effects that occur in chiral media in the presence of a magnetic field.[7] The synthesized chiral magnets are mainly inorganic or metallo-organic in nature.[8,9] It is observed that chiral magnets, in particular manganese silicide (MnSi), a cubic intermetallic compound that has no inversion symmetry, i.e., with a noncentrosymmetric crystal structure,[10] have attracted interest over the past few years, and they may one day reach a degree of functionality similar to that of chiral liquid crystals.[4] However, in the past few decades, the search for new ferromagnetic materials based on organic diradicals has generated tremendous interest.[11−13] Organic radicals[11] have been widely studied because of their versatile applicability in the field of magnetism[14] and their superconductivity,[15] spintronic properties,[16] photomagnetic behavior,[17] etc. In the case of organic diradicals, the magnetic interaction between two radical centers normally depends on the couplers that connect the radical centers.[18] A series of nitronylnitroxide (NN) diradicals with linear conjugated couplers have been studied by Ali and Datta, and they reported that the magnetic exchange coupling constant value decreases gradually with increasing coupler conjugation length.[19] It has been found that chains containing sp-hybridized carbon atoms are fascinating because of their unique linear structure and interesting physical properties.[20] Allenes (1,2-propadiene derivatives) make up an important class of compounds and have attracted a growing level of attention as interesting building blocks in synthetic organic chemistry.[21] Cumulenes with an odd number of carbon atoms have π-systems that are spatially orthogonal with each other; therefore, these systems contain a chiral axis, and their two pairs of substituents are in two perpendicular planes, giving rise to enantiomers.[22] Skibar et al. have synthesized cumulenes containing seven carbon atoms.[23] Januszewski et al. also have synthesized and predicted the properties of long cumulenes containing up to 10 carbon atoms.[24] Cumulenes are extensively used in molecular machines (nanomechanics), molecular wires (nanoelectronics), nonlinear optics, and molecular sensors because of their unique electronic structures.[25] It is found that among all conjugated oligomers, cumulene wires with an odd number of carbon atoms show the highest conductance with metallic-like ballistic transport behavior.[26]

Received: April 26, 2016
Published: June 10, 2016

DOI: 10.1021/acs.joc.6b00943
J. Org. Chem. 2016, 81, 5623−5630

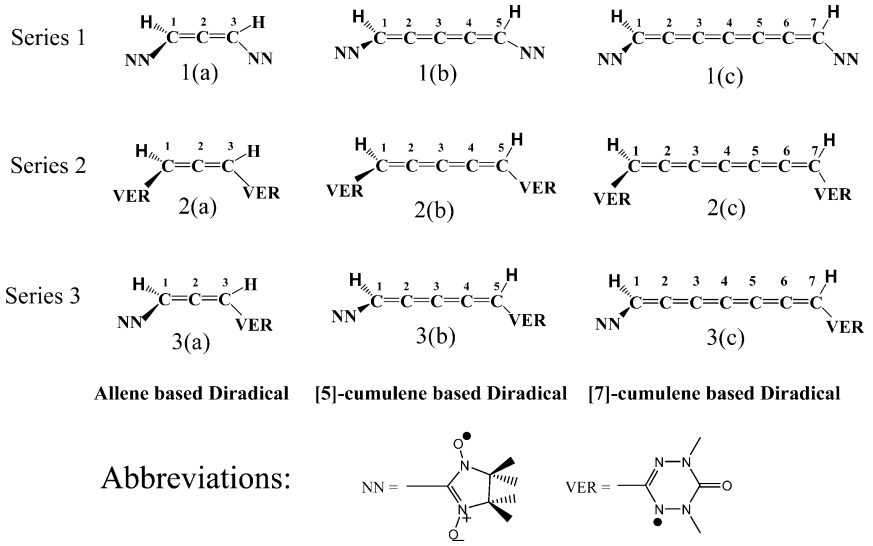

Figure 1. Allene- and cumulene-based diradicals. [5] and [7] indicate the number of carbon atoms in a coupler.

We have designed allene-based and cumulene-based (containing an odd number of carbon atoms) organic diradical systems that are shown in Figure 1 and have studied the magnetic properties of these diradicals in detail as an estimation of the intramolecular exchange coupling constant is necessary before a successful magnetic material based on organic diradicals or transition metal complexes can be synthesized. These designed molecules may be used as molecular building blocks for organic chiral magnetic solids.

2. THEORETICAL BACKGROUND

The magnetic exchange interaction between two magnetic sites 1 and 2 is generally expressed by the Heisenberg spin Hamiltonian $\hat{H} = -2J\hat{S}_1\hat{S}_2$, where $\hat{S}_1$ and $\hat{S}_2$ are the respective spin angular momentum operators and J is the exchange coupling constant between two magnetic centers. When J is positive, the high-spin state is lower in energy and the coupling is said to be ferromagnetic. A negative value of J is representative of antiferromagnetic interaction in the diradical, and a low-spin state is the ground state. For a diradical containing a single unpaired electron on each site, J can be represented as $E_{(S=1)} - E_{(S=0)} = -2J$.

Multiconfiguration approaches are suitable for describing pure spin states in an appropriate manner, but these methods are resource intensive and were not used in this work. To circumvent this issue, the broken symmetry (BS) approach by Noodleman et al.[27−30] in the density functional theory (DFT) framework is a more useful alternative for evaluating J that can eventually lead to an estimate of the energy of the diradical singlet. The ideal BS state is a weighted average of the singlet and the triplet and has an M_S equal to zero. The ideal triplet (T) state has $\langle S^2\rangle = 2$, whereas $\langle S^2\rangle = 1$ in the ideal BS state, which results in $E(\mathrm{BS}) - E(\mathrm{T}) = J$. However, in the actual calculation, approximate $\langle S^2\rangle$ values are obtained, and hence, the BS solution is often found to be spin-contaminated. Therefore, a correction is needed to calculate the coupling constant.

The spin-projected formula given by Yamaguchi[31−34] for the evaluation of the magnetic exchange coupling constant (J) is free from such spin contamination and applicable for both low and high overlap between magnetic orbitals, which can be written as $J = (E_{\mathrm{BS}} - E_{\mathrm{HS}})/(\langle S^2\rangle_{\mathrm{HS}} - \langle S^2\rangle_{\mathrm{BS}})$, where E_{BS}, E_{HS}, $\langle S^2\rangle_{\mathrm{BS}}$, and $\langle S^2\rangle_{\mathrm{HS}}$ are the energies and average spin square values for the BS and high-spin states, respectively.

3. COMPUTATIONAL STRATEGY

The molecular structures of all the diradicals have been fully optimized in each spin state by hybrid exchange-correlation functionals B3LYP and M06 in combination with the 6-311++G(d,p) basis set within the unrestricted formalism using the Gaussian09 quantum chemical package.[35] A broken symmetry (BS) singlet solution has been performed for mixing of the HOMO and the LUMO. The magnetic exchange coupling constant (J) value for each molecule has been estimated from the energies of triplet and BS states at the same level of theory using the spin-projected formula given by Yamaguchi.[31−34] To confirm the enantiomeric nature of our designed systems, we analyze the vibrational circular dichroism (VCD) spectra. Detailed analyses of geometrical parameters, the spin density distribution, and molecular orbital and natural orbital occupancies have been calculated with the optimized geometry. Details of the computational procedure are discussed in the Supporting Information.

4. RESULTS AND DISCUSSION

It is well-known that the two enantiomers of a chiral compound show optical rotation values of the same angles but in opposite directions in the presence of plane-polarized light. The absolute configuration of a chiral molecule can be determined from its VCD spectrum as the VCD spectra of the two enantiomers of a chiral molecule are equal in magnitude and opposite in sign.[2] Here we have tried to verify the enantiomeric relationship between our designed chiral molecules. For series 2 diradicals (Figure S1), calculated VCD spectra (Figure S2) confirm the stereochemistry as well as the enantiomeric relationship between them. The other diradicals (series 1 and series 3) have similar couplers; therefore, it is obvious that they will follow the same trend as series 2. The point here is that the form of the Hamiltonian guarantees the magnetic exchange coupling constant of the diradical-based chiral enantiomers to be equal in magnitude.

Magnetic Exchange Coupling Constant. The calculated magnetic exchange coupling constants of all the diradicals are listed in Table 1. The consistency of magnetic exchange coupling constant values has been confirmed using two different exchange-correlation functionals (B3LYP and M06). It is observed that although the values of coupling constants are different for different methods, they follow similar trends. From Table 1, it is

DOI: 10.1021/acs.joc.6b00943
J. Org. Chem. 2016, 81, 5623−5630

Table 1. Intramolecular Magnetic Exchange Coupling Constants (J) of Designed Diradicals

system	J (cm^{-1}) [B3LYP/6-311++G(d,p)]	J (cm^{-1}) [M06/6-311++G(d,p)]
1(a)	47.66	63.17
1(b)	99.09	146.28
1(c)	171.28	244.31
2(a)	15.30	22.96
2(b)	30.36	45.00
2(c)	53.17	86.95
3(a)	28.33	39.14
3(b)	55.84	78.62
3(c)	95.42	147.65

observed that with the increase in the chain length of the coupler from the allene-based diradical to the [5]-cumulene-based diradical, the magnetic exchange coupling constant increases almost 2-fold, and again upon the transition from the [5]-cumulene-based diradical to the [7]-cumulene-based diradical, the coupling constant further increases by approximately 2-fold, which contradicts the fact that the level of magnetic exchange decreases with an increase in the length of conjugated systems.[19] Therefore, it can be argued that there must be a major contribution of the coupler in the magnetic exchange pathway, and this observation demands a detailed investigation of the electronic structure of these couplers. If we compare the coupling constants of the same coupler with different radicals, we can see that the NN-based diradicals have highest coupling constant and VER-based diradicals have the lowest; a combination of two radicals NN and VER gives the coupling constant in between. Thus, we can conclude that the nitronyl nitroxide radical is more suitable for obtaining a coupling constant higher than that of verdazyl radical with allene and cumulene couplers. We have calculated the absolute energy values of the diradicals as $^1/_2(E^T_{NN} + E^T_{VER})$ and for mixed radical systems (see Table S3) and found that for allene-based diradicals the energy difference is as small as 0.00036 au and for longer cumulene there is no energy difference at all, which suggests that the interaction between radicals at the two ends of the molecules is not radical specific and decreases with an increase in the length of the carbon chain.

Spin Density Distribution. The spin density of the DFT-based approach can give us insight into the spin polarization mechanism for magnetic exchange coupling within the molecule. The exchange coupling constant between two magnetic sites largely depends on the delocalization of π-electron densities between them. Hence, to understand the anomalous increase in the magnitude of J, we have conducted spin density distribution analysis. Hund's rule-based spin density alternation rule[36,37] helps to predict the nature of magnetic interaction for diradicals with different couplers. Ferromagnetic exchange coupling takes place between two spin centers when they are connected by an even number of conjugated bonds, and antiferromagnetism occurs for an odd number of bonds.[36,37] The spin density distribution of the diradicals in their high-spin states (Figure S3) confirms that all these diradicals exhibit intramolecular ferromagnetic coupling.

The spin density on different atoms of a coupler and also the total spin density of a coupler in designed diradicals are listed in Table 2. Hermann et al. have proposed that cumulene-based systems with an even number of carbon centers, spin delocalization onto the chain increases as the length of the chain increases.[38] For our designed systems, it is also found that with an increase in the chain length of the coupler, the spin density on different atoms of the coupler and the total spin density on the coupler increase, which is quite contradictory from the concept that with an increase in the chain length of conjugated systems the spin density on the coupler decreases.[19] Hence, as argued in the previous subsection, there must be some special reason that facilitates spin polarization in such systems.

Spin Polarization. Chiral allene and cumulene couplers contain an even number of π-bonds in perpendicular planes; therefore, the two end π-bonds are perpendicular to each other. A close inspection of the spin density plot in Figure 2 for series 1

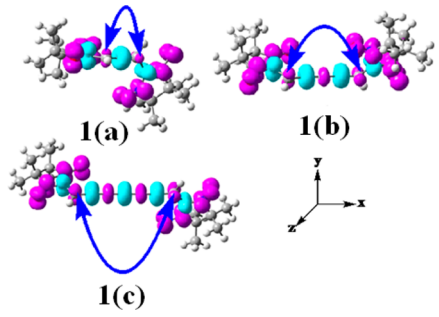

Figure 2. Spin density plot for the diradicals of series 1 in their triplet states [B3LYP/6-311++G(d,p)] (iso value of 0.004), in which magenta and sky colors represent the α and β spins, respectively. The blue arrow represents two end carbons of the coupler.

diradicals points to the fact that the spin density distributions of π-electrons of two end carbon atoms of the coupler are individually directed along two Cartesian axes (y and z directions), but for rest of the carbon atoms within the coupler, spin polarization of π-electrons is along both the y and z directions collectively, causing a

Table 2. Spin Density Distribution on Each Atom of the Coupler and Total Spin Density of the Coupler in Designed Diradicals in Their Triplet State [B3LYP/6-311++G(d,p)]

	spin density on different atoms of the coupler							
system	C1	C2	C3	C4	C5	C6	C7	total spin density
1(a)	0.0768	−0.2655	0.0768	–	–	–	–	−0.1120
1(b)	0.1072	−0.2664	0.1572	−0.2665	0.1071	–	–	−0.1614
1(c)	0.1501	−0.3004	0.2041	−0.3196	0.2041	−0.3004	0.1501	−0.2120
2(a)	0.0616	−0.141	0.0616	–	–	–	–	−0.0177
2(b)	0.0831	−0.1341	0.0652	−0.1341	0.0831	–	–	−0.0366
2(c)	0.1223	−0.1659	0.0899	−0.1396	0.0899	−0.1659	0.1223	−0.0470
3(a)	0.0638	−0.1862	0.0683	–	–	–	–	−0.0541
3(b)	0.1025	−0.2095	0.114	−0.1969	0.0953	–	–	−0.0946
3(c)	0.1437	−0.2437	0.1711	−0.2488	0.1469	−0.2316	0.1362	−0.1262

DOI: 10.1021/acs.joc.6b00943
J. Org. Chem. 2016, 81, 5623−5630

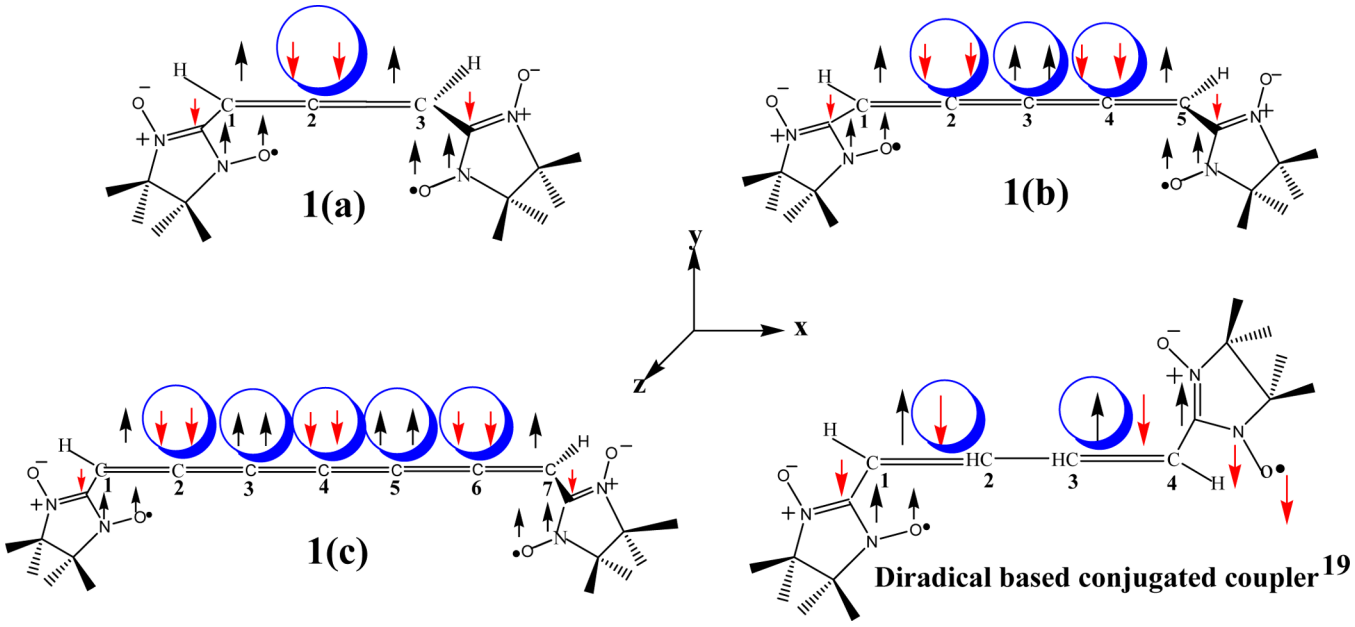

Figure 3. Spin polarization of π-electrons within the coupler (for series 1).

high level of accumulation of spin density for the middle carbons of the coupler chain. A plausible mechanistic pathway of spin polarization within the coupler is shown in Figure 3.

To explain the increase in spin density upon addition of a carbon center within the coupler, and simultaneously to explain the contradictory behavior of spin polarization in cumulenes compared to that of conjugated systems (i.e., alternating σ- and π-bonds), a detailed investigation of the mechanistic pathway of spin polarization was conducted. Figure 3 shows that the two end carbons in the allene-based diradical contain one π-bonding electron on each of them, but the central carbon contains two π-bonding electrons in two different p orbitals at a time. Therefore, for allene-based diradicals, spin polarization is greater in the middle carbon than in the end carbons. Now upon comparison of the allene-based diradical with the [5]-cumulene-based diradical, we find that the former contains only one carbon with two π-electrons in the central region of the coupler but later contains three carbons with two π-electrons on each. As a result, the [5]-cumulene-based diradical has higher level of accumulation of spin density on each carbon of the coupler compared to that of the allene-based diradical. A similar trend in the [7]-cumulene-based diradical is also observed. Thus, one can surmise that spin polarization increases considerably with an increase in the number of carbon centers of the coupler in cumulene systems.

Upon comparison of the spin density of cumulene with that of the conjugated coupler, it is found that for conjugated coupler-based diradicals, each carbon atom of the coupler contains one π-electron on each and no such enhancement of spin polarization occurs; moreover, a decrease in spin density with an increase in the chain length of the coupler is observed as the distance between the radical centers increases. Figure 4 is a plot of the coupling constant versus the distance between the radical centers that clearly shows the variation of the coupling constant with distance.

Therefore, a high level of accumulation of spin density within the coupler overcomes the distance factor between the radical centers in the case of cumulene-based diradicals, and higher magnetic exchange coupling results from the increase in the length of the coupler.

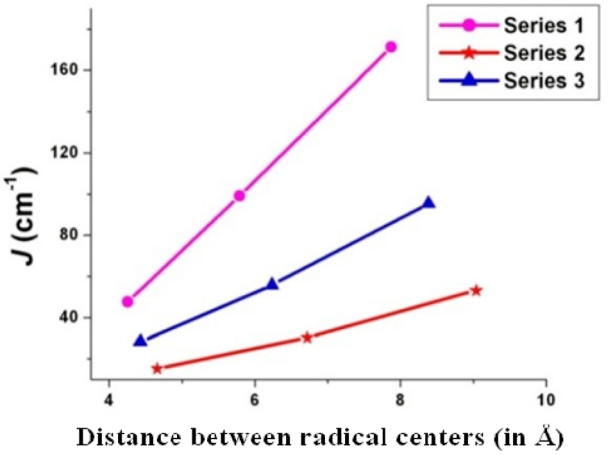

Figure 4. Plot of the magnetic exchange coupling constant vs distance between the radical centers [B3LYP/6-311++G(d,p)].

Molecular Structures. A small change in molecular structure can lead to a drastic change in the magnetic coupling constant.[39] Therefore, it is important to study the molecular structure of the allene- and cumulene-based diradicals to understand their magnetic behavior. The optimized geometrical parameters of our designed diradicals are reported in Tables 3 and 4.

The most important structural aspect is the bond distance alteration of the cumulene moiety. Our calculations predict a distinct alternation of adjacent C═C bonds, and the first and last bond lengths for all the diradicals are approximately close to the double bond length in ethylene (132 pm). The central double bond distance in [5]-cumulene-based diradicals is approximately 127 pm, and their values are between the double bond length in ethylene (132 pm) and the triple bond length in acetylene (121.2 pm). The central bond distances for [7]-cumulene are also approximately 128 pm, and double bond lengths elsewhere in the bridge chain equal 126 pm and their values between the double bond length in ethylene (132 pm) and the triple bond length in acetylene (121.2 pm). When two different groups are included, all the double bond lengths become unequal (see series 3). These

DOI: 10.1021/acs.joc.6b00943
J. Org. Chem. 2016, 81, 5623−5630

Table 3. Bond Distances between Two Atoms and Average Bond Distances of the Couplers for the Designed Diradicals in their Triplet State [B3LYP/6-311++G(d,p)][a]

	bond distance										
system	C1═C2	C2═C3	C3═C4	C4═C5	C5═C6	C6═C7	average bond distance of coupler	distance between C1 and L	distance between C3 and R	distance between C5 and R	distance between C7 and R
1(a)	131.1	131.1	–	–	–	–	131.1	143.8	143.8	–	–
1(b)	132.6	127.0	127.0	132.6	–	–	129.8	142.8	–	142.8	–
1(c)	133.3	126.4	128.1	128.1	126.4	133.3	129.3	142.3	–	–	142.3
2(a)	130.7	130.7	–	–	–	–	130.7	147.3	147.3	–	–
2(b)	131.9	127.2	127.2	131.9	–	–	129.5	146.6	–	146.6	–
2(c)	132.3	126.7	128.0	128.0	126.7	132.3	129.0	146.2	–	–	146.2
3(a)	131.3	130.5	–	–	–	–	130.1	144.0	147.2	–	–
3(b)	132.6	126.9	127.3	131.8	–	–	129.7	142.9	–	146.5	–
3(c)	133.3	126.3	128.3	127.9	126.8	132.4	129.2	142.3	–	–	146.2

[a]All bonds are in picometers. L is the connecting atom of the left radical center and R the connecting atom of the right radical center.

Table 4. Bond Angles (degrees) for the Couplers in the Diradicals in Series 1−3 in Their Triplet State [B3LYP/6-311++G(d,p)]

system	∠c1−c2−c3	∠c2−c3−c4	∠c3−c4−c5	∠c4−c5−c6	∠c5−c6−c7
1(a)	173.87	–	–	–	–
1(b)	174.35	177.97	174.35	–	–
1(c)	174.33	178.42	179.8	178.41	174.33
2(a)	177.92	–	–	–	–
2(b)	178.12	179.76	178.11	–	–
2(c)	178.13	179.88	179.95	179.87	178.14
3(a)	175.75	–	–	–	–
3(b)	174.54	178.49	178.23	–	–
3(c)	174.44	178.59	179.76	179.83	178.11

different bond lengths are indicative of electronically different bonding situations.

Another important point is that the average C−C bond length tends to decrease with an increase in cumulene chain length in a particular series, as for series 1 the values are 131.1, 129.8, and 129.3 pm for systems 1(a)−1(c), respectively, and this is closer to a double bond distance, as expected. It is observed that with a decrease in the average bond length in each series, there is the possibility of increasing the s-character of the coupler. The higher the s-character, the greater the electronegativity of that atom and the greater the likelihood of localizing the spin density on that atom, which facilitates the higher spin densities on the coupler with an increase in length. From Table 3, it is also clear that with an increase in the length of the coupler the distance between the carbon atoms of the coupler and the radical centers decreases in each series; therefore, the level of conjugation between the coupler and the radical center increases. Thus, ultimately, a better π-interaction results with an increase in the chain length of the coupler.

The computed bond angles between the carbon atoms in the coupler are listed in Table 4. It is confirmed that the bond angle of the coupler deviates from the exact angle of allene (180°); hence, they are the systems with a nonlinear C═C═C framework and are characterized by slightly deviated orthogonal π-bonds. This bending is greater in the case of allene-based diradicals than in the case of cumulene-based diradicals. For this, the allene π-system is significantly disturbed, and the central carbon atom is no longer sp-hybridized as in typical all-carbon allenes. Now, via comparison of diradical-substituted allene with their higher homologue, it is found that with an increase in the chain length the middle allene counterpart goes nearly 180° [e.g, for 1(a), ∠c1−c2−c3 = 173.87°; for 1(b), ∠c2−c3−c4 = 177.97°; for 1(c), ∠c3−c4−c5 = 179.8°]. Hence, there is relatively strong π-interaction with increasing chain length in each series, and the coupling constant increases accordingly.

Molecular Orbital Analysis. The shape of molecular orbitals plays a major role in determining the magnetic properties of the diradicals, electronic transport, etc.[40] Frontier molecular orbitals (FMOs) of all the axially chiral allene- and cumulene-based diradicals are presented in Figure 5. According to Borden and co-workers when the nonbonding molecular orbitals of a diradical have no atoms in common, i.e., disjointed in nature, the diradicals favor the antiferromagnetic state as the ground state. The nondisjointed SOMOs favor the ferromagnetic ground state. From Figure 5, one can see that α-SOMOs of diradicals in series 1 and 2 are nondisjointed and α-SOMOs of diradicals in series 3 are disjointed, although all the diradicals are ferromagnetic in nature. We have conducted molecular orbital analysis of diradicals 1 and 2 with varying geometries to check the stability of the nondisjointed nature of the SOMOs and found that the SOMOs are unaltered upon structural changes (Figure S4). Thus, Borden's analogy,[41,42] which is derived for alternant hydrocarbons, does not fit for the disjointed diradicals in series 3. Thus, it may be surmised that Borden's analogy, which is derived for alternant hydrocarbons, does not fit for these diradicals, and such systems follow a different mechanism for magnetic interaction.

The molecular orbital analysis of the BS determinant of an allene-based diradical (see Figure S5) shows that for 1(a) and 2(a) diradicals, the α-HOMO and β-HOMO are on the two individual radical centers. However, α-SOMOs of the triplet state for those diradicals are distributed collectively on two radical centers, but for series 3 diradicals [(a)], the shape of the α-HOMO and β-HOMO of the BS determinant and α-SOMOs of the triplet state are the same. Therefore, the SOMOs of the BS determinant and triplet state are not exactly the same for all the diradicals but are distributed only over radical centers.

Mechanism of Magnetic Interaction. Molecular orbitals play an important role in understanding the magnetic coupling between two radical centers. It is known that the SOMOs are mainly responsible for magnetic interaction in diradicals through itinerant exchange[41−44] and the small SOMO−SOMO gap or degenerate SOMOs produce a strong magnetic exchange coupling constant. The SOMO−SOMO energy gap and the HOMO−LUMO energy gap for the designed diradicals are listed in Table 5. The energy of FMOs is given in Table S4. We observe

DOI: 10.1021/acs.joc.6b00943
J. Org. Chem. 2016, 81, 5623−5630

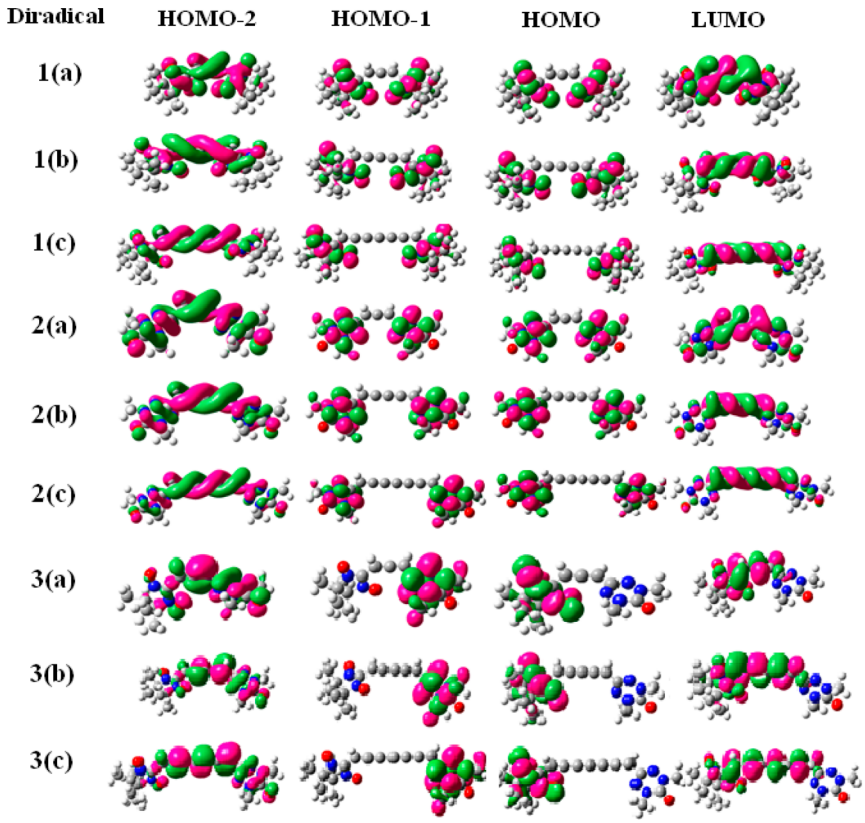

Figure 5. Spatial distribution of molecular orbitals of all the diradicals in their triplet states [B3LYP/6-311++G(d,p)] (iso value of 0.02), in which green and pink colors represent the different phase of the orbital coefficients.

Table 5. Energy Differences between SOMO1 $(HOMO)_\alpha$–SOMO2 $(HOMO-1)_\alpha$ (ΔE_{SS}) and $HOMO_\alpha$–$LUMO_\alpha$ (ΔE_{HL}) and Magnetic Exchange Coupling Constants (J) in Their Triplet State [B3LYP/6-311++G(d,p)]

system	ΔE_{SS} (eV)	ΔE_{HL} (eV)	J (cm^{-1})
1(a)	0.01	3.71	47.66
1(b)	0.00	3.03	99.09
1(c)	0.00	2.64	171.28
2(a)	0.02	4.14	15.30
2(b)	0.00	3.35	30.36
2(c)	0.00	2.85	53.17
3(a)	0.13	3.72	28.33
3(b)	0.13	3.00	55.84
3(c)	0.09	2.79	95.42

from the values listed in Table 5 that for series 1 and 2, the two SOMOs are almost degenerate, although they have different J values in each series. Another interesting point is that for diradicals 3(a) and 3(b) the SOMO–SOMO gap is largest and equal in magnitude but shows different J values. Therefore, the SOMO–SOMO gap is not the only guiding factor in determining the extent of magnetic interaction; there must be some other factor that guides magnetic exchange. In a couple of our recent works, we have found that the SOMO–SOMO gap is not responsible for the strength of magnetic coupling but rather that the HOMO–LUMO gap plays a more important role.[39,45,46] If we focus on the difference in energy between the HOMO and LUMO in this study, it has been found that upon going from the allene-based diradical to its higher homologue ([5]- and [7]-cumulene) in each series, there is a smooth decrease in the HOMO–LUMO energy gap. Hermann et al. also have shown that the α-HOMO–α-LUMO gap decreases with an increase in the carbon chain lengths of cumulene-based systems containing an even number of carbon centers.[38] Therefore, we can conclude that diradicals with a small HOMO–LUMO gap facilitate a strong magnetic coupling constant, and diradicals based on allene and cumulene couplers with a small HOMO–LUMO gap will be promising candidates for designing chiral organic magnetic molecules.

Our designed diradicals based on allene and [5]- and [7]-cumulene couplers (containing an odd number of carbon atoms) have two π-conjugations that are mutually perpendicular to each other. Imamura and Aoki have proposed that polyyne has two π-conjugated systems mutually perpendicular to each other and both the π-conjugations have a tendency to follow a bond alternation that is the origin of a competition between them.[47−49] With an increase in the length of the polyyne chain, a remarkable transition in the molecular structure takes place from an almost equidistant bond structure to an intensely alternating bond structure, which causes an increase in the HOMO level and a decrease in the LUMO level. As a result, there is a sudden decrease in the HOMO–LUMO gap with an increase in the length of the polyyne chains. The orbital phases of two mutually perpendicular π-conjugations for our designed diradicals are shown in Figure 6.

For our designed diradicals, $HOMO_\alpha$ and $(HOMO-1)_\alpha$ are the nonbonding molecular orbitals; therefore, the energy of LUMO decreases and the energy of HOMO−2 increases remarkably (shown in Figure 7), which satisfies the proposal of Imamura et al.[47−49] As a result, there is a decrease in the $HOMO_\alpha$–$LUMO_\alpha$ and $(HOMO-2)_\alpha$–$(HOMO-1)_\alpha$ energy gaps.

DOI: 10.1021/acs.joc.6b00943
J. Org. Chem. 2016, 81, 5623−5630

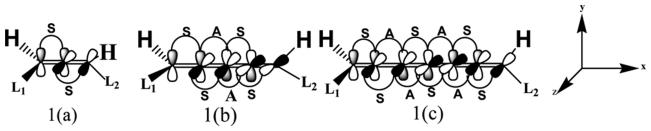

Figure 6. Structure of allene-based diradical and cumulene-based diradical with phases of HOMO−2. S indicates symmetric and A antisymmetric in the phase of MO. L_1 and L_2 are the left and right radical centers, respectively.

To determine the role of LUMO in the magnetic exchange coupling constant, we have computed the electron occupation in LUMO and HOMO−2 and SOMOs (Table 6).

From Table 6, we can see that LUMOs have a considerable amount of occupation. Therefore, we can assume that the LUMO takes part in the exchange mechanism. Here, we can see that in case of diradicals (c) in all series 1−3, the LUMO has the highest level of occupation in their respective series. The higher level of occupation in the LUMO favors strong intramolecular magnetic exchange coupling between the radical centers. Therefore, there is a correlation between the LUMO occupation and magnetic exchange coupling constant.

5. CONCLUSION

All the designed diradicals have ferromagnetic interaction that is strengthened upon addition of chiral centers within the coupler. Spin density distribution analysis shows that with an increase in the length of the coupler, enhancement of spin polarization along the coupler takes place and the probability of localizing the spin density on each chiral center increases. Addition of chiral centers within the coupler lowers the energy of LUMO; a smaller HOMO−LUMO gap facilitates a stronger magnetic coupling, and a higher magnetic exchange coupling constant (J) results. From natural orbital occupancies, we found that with an increase in the chain length of the chiral coupler the occupancy of LUMO increases. Furthermore, nonapplicability of Borden's rule indicates that a good way of predicting the ground state of the diradical systems having allene and [n]-cumulene coupler should be by Hund's rule-based spin density alternation. A close inspection of J values shows that NN stands for a better choice of radical center over VER and mixed radicals. Thereby, we expect that this trend might inspire synthetic chemists to synthesize NN-based chiral magnetic molecules with strong ferromagnetic interaction. The diradicals with an [n]-cumulene coupler with n being an even number will show antiferromagnetic behavior according to the spin alternation rule. These antiferromagnetic diradicals will be discussed elsewhere.

Table 6. Natural Orbital Occupation of the Diradicals in the Triplet State [B3LYP/6-311++G(d,p)]

system	HOMO−2	HOMO−1	HOMO	LUMO
1(a)	1.968	1.0	1.0	0.032
1(b)	1.952	1.0	1.0	0.048
1(c)	1.924	1.0	1.0	0.073
2(a)	1.990	1.0	1.0	0.009
2(b)	1.986	1.0	1.0	0.014
2(c)	1.980	1.0	1.0	0.020
3(a)	1.969	1.0	1.0	0.031
3(b)	1.954	1.0	1.0	0.046
3(c)	1.931	1.0	1.0	0.069

■ ASSOCIATED CONTENT

Supporting Information

The Supporting Information is available free of charge on the ACS Publications website at DOI: 10.1021/acs.joc.6b00943.

R and *S* configurations and VCD spectra of series 2 diradicals, exchange coupling constants of the enantiomers, energy and *J* values of the diradicals using different functionals (B3LYP and M06), spin density distribution using B3LYP, spatial distribution of molecular orbitals of the diradicals with varying geometries, molecular orbital of the diradicals in their broken symmetry state, energies of FMOs of all diradicals, and coordinates of the optimized geometries (PDF)

■ AUTHOR INFORMATION

Corresponding Author

*Phone: +91-9434228745. E-mail: anirbanmisra@yahoo.com.

Notes

The authors declare no competing financial interest.

■ ACKNOWLEDGMENTS

This work is supported by DST, India. S.S. is thankful to Sonderforschungsbereich 668, University of Hamburg, for a

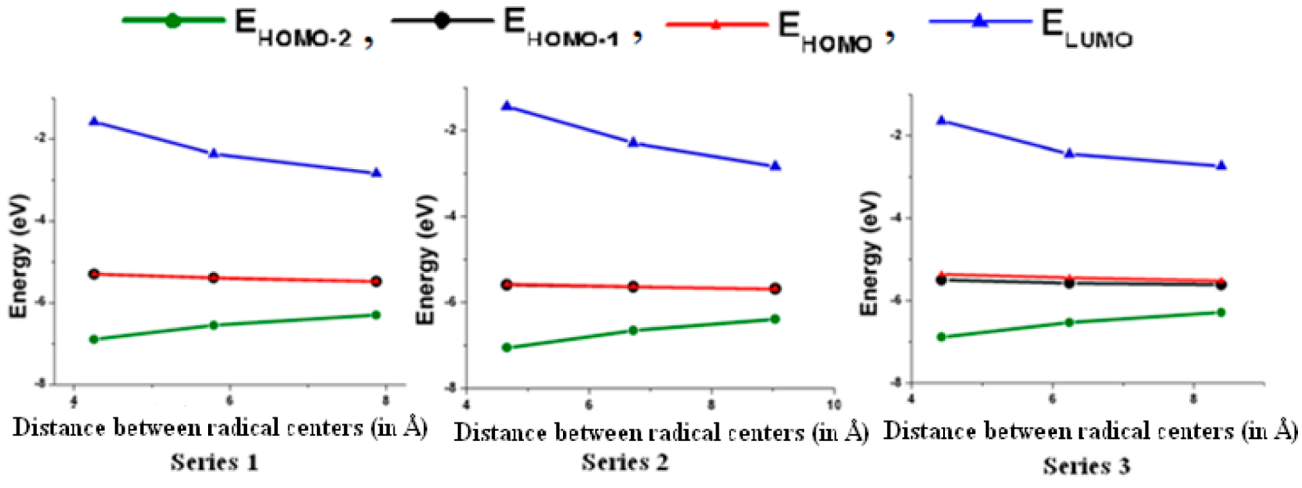

Figure 7. Plot of energy vs distance between radical centers for series 1−3 in their triplet state [B3LYP/6-311++g(d,p)].

DOI: 10.1021/acs.joc.6b00943
J. Org. Chem. 2016, 81, 5623−5630

postdoctoral fellowship. We are also thankful to the Hamburg regional computing center (RRZ) for computational resources.

REFERENCES

(1) Nguyen, L. A.; He, H.; Pham-Huy, C. *Int. J. Biomed. Sci.* **2006**, *2*, 85−100.
(2) Stephens, P. J.; Devlin, F. J.; Pan, J.-J. *Chirality* **2008**, *20*, 643−663.
(3) Galán-Mascarós, J. R.; Coronado, E.; Goddard, P. A.; Singleton, J.; Coldea, A. I.; Wallis, J. D.; Coles, S. J.; Alberola, A. *J. Am. Chem. Soc.* **2010**, *132*, 9271.
(4) Pappas, C. *Physics* **2012**, *5*, 28.
(5) Train, C.; Gheorghe, R.; Krstic, V.; Chamoreau, L.-M.; Ovanesyan, N. S.; Rikken, G. L. J. A.; Gruselle, M.; Verdaguer, M. *Nat. Mater.* **2008**, *7*, 729−734.
(6) Togawa, Y.; Koyama, T.; Takayanagi, K.; Mori, S.; Kousaka, Y.; Akimitsu, J.; Nishihara, S.; Inoue, K.; Ovchinnikov, A. S.; Kishine, J. *Phys. Rev. Lett.* **2012**, *108*, 107202.
(7) Wagnière, G. H. *Chem. Phys.* **1999**, *245*, 165−173.
(8) Bordács, S.; Kézsmárki, I.; Szaller, D.; Demko, L.; Kida, N.; Murakawa, H.; Onose, Y.; Shimano, R.; Rõõm, T.; Nagel, U.; Miyahara, S.; Furukawa, N.; Tokura, Y. *Nat. Phys.* **2012**, *8*, 734.
(9) Minguet, M.; Luneau, D.; Paulsen, C.; Lhotel, E.; Gorski, A.; Waluk, J.; Amabilino, D. B.; Veciana, J. *Polyhedron* **2003**, *22*, 2349−2354.
(10) (a) Ishikawa, I.; Tajima, K.; Bloch, D.; Roth, M. *Solid State Commun.* **1976**, *19*, 525−528. (b) Yu, X. Z.; Onose, Y.; Kanazawa, N.; Park, J. H.; Han, J. H.; Matsui, Y.; Nagaosa, N.; Tokura, Y. *Nature* **2010**, *465*, 901−904.
(11) Kahn, O. *Molecular Magnetism*; VCH: New York, 1993.
(12) Coronado, E.; Delhaè, P.; Gatteschi, D. *Molecular magnetism: From molecular assemblies to devices*; Miller, J. S., Ed.; NATO ASI Series E321; Kluwer: Dordrecht, The Netherlands, 1996; Vol. *321*.
(13) Benelli, C.; Gatteschi, D. *Chem. Rev.* **2002**, *102*, 2369−2387.
(14) Lahti, P. M. *Magnetic Properties of Organic Materials*; Marcel Dekker: New York, 1999.
(15) (a) Kobayashi, H.; Kobayashi, A.; Cassoux, P. *Chem. Soc. Rev.* **2000**, *29*, 325−333. (b) Uji, S.; Shinagawa, H.; Terashima, T.; Yakabe, T.; Terai, Y.; Tokumoto, M.; Kobayashi, A.; Tanaka, H.; Kobayashi, H. *Nature* **2001**, *410*, 908−910.
(16) (a) Prinz, G. A. *Science* **1998**, *282*, 1660−1663. (b) Emberly, E. G.; Kirczenow, G. *Chem. Phys.* **2002**, *281*, 311−324.
(17) (a) Matsuda, K.; Matsuo, M.; Irie, M. *J. Org. Chem.* **2001**, *66*, 8799−8803. (b) Tanifuji, N.; Irie, M.; Matsuda, K. *J. Am. Chem. Soc.* **2005**, *127*, 13344−13353.
(18) (a) Bhattacharya, D.; Misra, A. *J. Phys. Chem. A* **2009**, *113*, 5470−5475. (b) Bhattacharya, D.; Shil, S.; Misra, A.; Klein, D. J. *Theor. Chem. Acc.* **2010**, *127*, 57−67. (c) Bhattacharya, D.; Shil, S.; Panda, A.; Misra, A. *J. Phys. Chem. A* **2010**, *114*, 11833−11841.
(19) Ali, Md. E.; Datta, S. N. *J. Phys. Chem. A* **2006**, *110*, 2776−2784.
(20) (a) Tobe, Y.; Wakabayashi, T. In *Acetylene Chemistry: Chemistry, Biology, and Material Science*; Diederich, F., Stang, P. J., Tykwinski, R. R., Eds.; Wiley-VCH: Weinheim, Germany, 2005; pp 387−426. (b) Chalifoux, W. A.; Tykwinski, R. R. *Chem. Rec.* **2006**, *6*, 169−182. (c) Shi Shun, A. L. K.; Tykwinski, R. R. *Angew. Chem., Int. Ed.* **2006**, *45*, 1034−1057. (d) Raton, B. *Polyynes: Synthesis, Properties, and Applications*; Cataldo, F., Ed.; Taylor & Francis: Boca Raton, FL, 2005.
(21) Taylor, D. R. *Chem. Rev.* **1967**, *67*, 317.
(22) Hendon, C. H.; Tiana, D.; Murray, A. T.; Carbery, D. R.; Walsh, A. *Chem. Sci.* **2013**, *4*, 4278−4284.
(23) Skibar, W.; Kopacka, H.; Wurst, K.; Salzmann, C.; Ongania, K. H.; Fabrizi de Biani, F.; Zanello, P.; Bildstein, B. *Organometallics* **2004**, *23*, 1024−1041.
(24) (a) Januszewski, J. A.; Tykwinski, R. R. *Chem. Soc. Rev.* **2014**, *43*, 3184−3203. (b) Januszewski, J. A.; Wendinger, D.; Methfessel, C. D.; Hampel, F.; Tykwinski, R. R. *Angew. Chem., Int. Ed.* **2013**, *52*, 1817−1821.
(25) Gu, X.; Kaiser, R. I.; Mebel, A. M. *ChemPhysChem* **2008**, *9*, 350−369.
(26) Prasongkit, J.; Grigoriev, A.; Wendin, G.; Ahuja, R. *Phys. Rev. B: Condens. Matter Mater. Phys.* **2010**, *81*, 115404.
(27) Noodleman, L. *J. Chem. Phys.* **1981**, *74*, 5737−5743.
(28) Noodleman, L.; Baerends, E. J. *J. Am. Chem. Soc.* **1984**, *106*, 2316−2327.
(29) Noodleman, L.; Davidson, E. R. *Chem. Phys.* **1986**, *109*, 131−143.
(30) Noodleman, L.; Peng, C. Y.; Case, D. A.; Mouesca, J.-M. *Coord. Chem. Rev.* **1995**, *144*, 199−244.
(31) Yamaguchi, K.; Fukui, H.; Fueno, T. *Chem. Lett.* **1986**, *15*, 625−628.
(32) Yamaguchi, K.; Takahara, Y.; Fueno, T.; Nasu, K. *Jpn. J. Appl. Phys.* **1987**, *26*, L1362−L1364.
(33) Yamaguchi, K.; Jensen, F.; Dorigo, A.; Houk, K. N. *Chem. Phys. Lett.* **1988**, *149*, 537−542.
(34) Yamaguchi, K.; Takahara, Y.; Fueno, T.; Houk, K. N. *Theor. Chim.Acta* **1988**, *73*, 337−364.
(35) Frisch, M. J.; Trucks, G. W.; Schlegel, H. B.; Scuseria, G. E.; Robb, M. A.; Cheeseman, J. R.; Scalmani, G.; Barone, V.; Mennucci, B.; Petersson, G. A.; Nakatsuji, H.; Caricato, M.; Li, X.; Hratchian, H. P.; Izmaylov, A. F.; Bloino, J.; Zheng, G.; Sonnenberg, J. L.; Hada, M.; Ehara, M.; Toyota, K.; Fukuda, R.; Hasegawa, J.; Ishida, M.; Nakajima, T.; Honda, Y.; Kitao, O.; Nakai, H.; Vreven, T.; Montgomery, J. A., Jr.; Peralta, J. E.; Ogliaro, F.; Bearpark, M.; Heyd, J. J.; Brothers, E.; Kudin, K. N.; Staroverov, V. N.; Kobayashi, R.; Normand, J.; Raghavachari, K.; Rendell, A.; Burant, J. C.; Iyengar, S. S.; Tomasi, J.; Cossi, M.; Rega, N.; Millam, M. J.; Klene, M.; Knox, J. E.; Cross, J. B.; Bakken, V.; Adamo, C.; Jaramillo, J.; Gomperts, R.; Stratmann, R. E.; Yazyev, O.; Austin, A. J.; Cammi, R.; Pomelli, C.; Ochterski, J. W.; Martin, R. L.; Morokuma, K.; Zakrzewski, V. G.; Voth, G. A.; Salvador, P.; Dannenberg, J. J.; Dapprich, S.; Daniels, A. D.; Farkas, Ö.; Foresman, J. B.; Ortiz, J. V.; Cioslowski, J.; Fox, D. J. *Gaussian09*; Gaussian, Inc.: Wallingford, CT, 2009.
(36) Trindle, C.; Nath Datta, S. N. *Int. J. Quantum Chem.* **1996**, *57*, 781−799.
(37) Trindle, C.; Datta, S. N.; Mallik, B. *J. Am. Chem. Soc.* **1997**, *119*, 12947−12951.
(38) Herrmann, C.; Neugebauer, J.; Gladysz, J. A.; Reiher, M. *Inorg. Chem.* **2005**, *44*, 6174−6182.
(39) Shil, S.; Herrmann, C. *Inorg. Chem.* **2015**, *54*, 11733−11740.
(40) Browne, W. R.; Hage, R.; Vos, J. G. *Coord. Chem. Rev.* **2006**, *250*, 1653−1668.
(41) Borden, W. T.; Davidson, E. R. *J. Am. Chem. Soc.* **1977**, *99*, 4587−4594.
(42) Borden, W. T.; Davidson, E. R. *Acc. Chem. Res.* **1981**, *14*, 69−76.
(43) Constantinides, C. P.; Koutentis, P. A.; Schatz, J. *J. Am. Chem. Soc.* **2004**, *126*, 16232−16241.
(44) Zhang, G.; Li, S.; Jiang, Y. *J. Phys. Chem. A* **2003**, *107*, 5573−5582.
(45) Shil, S.; Roy, M.; Misra, A. *RSC Adv.* **2015**, *5*, 105574−105582.
(46) Bhattacharya, D.; Shil, S.; Misra, A.; Bytautas, L.; Klein, D. J. *Phys. Chem. Chem. Phys.* **2015**, *17*, 14223−14237.
(47) Aoki, Y.; Imamura, A. *J. Chem. Phys.* **1995**, *103*, 9726.
(48) Imamura, A.; Aoki, Y. *Int. J. Quantum Chem.* **2006**, *106*, 1924−1933.
(49) Imamura, A.; Aoki, Y. *Int. J. Quantum Chem.* **2013**, *113*, 423−427.

DOI: 10.1021/acs.joc.6b00943
J. Org. Chem. 2016, 81, 5623−5630